ACCOUNTS
of chemical research

Nanoelectronic Heterodyne Sensor: A New Electronic Sensing Paradigm

Published as part of the Accounts of Chemical Research special issue "Nanoelectrochemistry".

Girish S. Kulkarni,[†,‡] Wenzhe Zang,[†] and Zhaohui Zhong*,[†]

[†]Department of Electrical Engineering and Computer Science, University of Michigan, 1301 Beal Ave, Ann Arbor, Michigan 48109, United States

[‡]Arborsense, Inc., 1600 Huron Pkwy, Bldg. 520, Ann Arbor, Michigan 48109, United States

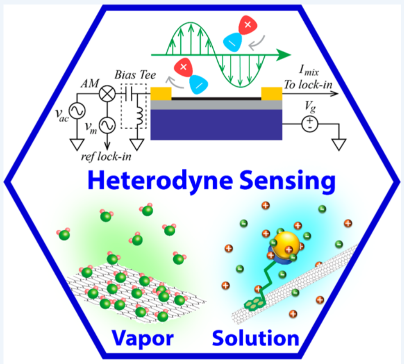

CONSPECTUS: Nanoelectronic devices based on nanomaterials such as nanowires, carbon nanotubes, graphene, and other 2D nanomaterials offer extremely large surface-to-volume ratios, high carrier mobility, low power consumption, and high compatibility for integration with modern electronic technologies. These distinct advantages promise great potential for nanoelectronic devices as next generation chemical and biological sensors. Currently, majority of existing nanoelectronic sensors are direct current (DC) sensors, which rely ubiquitously on detection of conductance change associated with molecular adsorption. However, despite the simplicity of the conventional DC sensing technology, it also has severe limitations such as the Debye screening effect in ionic solutions, and the speed-sensitivity trade-off for the detection of charge-neutral molecules. Hence, the development of nanoelectronic sensors calls for new sensing platform technologies that can truly showcase the advantages of electronic sensors.

In this Account, we will summarize recent efforts from our group on the development of a new electronic sensing paradigm, the nanoelectronic heterodyne sensors. Unlike conventional charge-detection based sensors, the heterodyne sensor explores the frequency mixing response between molecular dipoles and a nanoscale transistor. As an example, we first discuss the capability of heterodyne sensing in gas sensing applications by using graphene devices. Rapid (down to 0.1 s) and sensitive (down to 1 ppb) detection of a wide range of vapor analytes is achieved, representing orders of magnitude improvement over state-of-the-art nanoelectronic sensors. Furthermore, the heterodyne sensing technique enables electrical probing and tuning of the noncovalent physisorption of polar molecules on graphene surface for the first time. These results provide insight into small molecule-nanomaterial interaction dynamics and signify the ability to electrically tailor interactions, which can lead to rational designs of complex chemical processes for catalysis and drug discovery. Finally, we discuss the application of heterodyne sensing in solution for chemical and biological sensors by using carbon nanotube devices. The fundamental ionic screening effect can be mitigated by operating carbon nanotube field effect transistor as a heterodyne biosensor. Electrical detection of streptavidin binding to biotin in 100 mM buffer solution can be achieved at a frequency beyond 1 MHz. The results should promise a new biosensing platform for point-of-care detection, where biosensors functioning directly in physiologically relevant condition are desired.

■ INTRODUCTION

A gamut of areas including defense and homeland security,[1] industrial and environmental monitoring,[2] clinical screening and medical diagnosis,[3,4] genomics,[5] and drug delivery[6] need sensors capable of monitoring low concentrations of molecules while maintaining stringent requirements on sensor's speed, size, and long-term stability.[7−9] Nanoelectronic platforms based on 1-D and 2-D nanoscale materials not only meet the above criteria but also have size scales comparable to target analytes of interest, e.g., viruses, proteins, DNA, and volatile chemicals, thereby promising detection down to single molecule level.[10−12] This, in addition to properties like chemical robustness, electrical read-out, low-power consumption, and ease-of-integration with microfabrication technology,[13−16] has consequently led to a lot of exciting work on nanoelectronic chemical and biological sensors. Researchers have demonstrated parts per billion (ppb) sensitivities for gas molecules[17] and femtomolar sensitivities[18,19] for biological species. Further, a wide range of molecules including proteins,[19] viruses,[20] organic[21] and inorganic[22] molecules, ions,[23] and polar and nonpolar analytes[24] have been successfully detected on nanoelectronic platforms. For example, CNTs and nanowires have been used to detect vapor analytes like amines,[21] nerve agents,[24] alcohols,[25] and *n*-alkanes[25] with parts per billion sensitivities. Similarly, 2-D materials—graphene,[26−28] MoS_2,[29] and phosphorene[30] have also been exploited for vapor sensing applications with high sensitivity. In solution based detection, the Lieber group has demonstrated the versatility of silicon nanowire sensors in detecting ions,[23] cancer markers,[19] pH

Received: June 29, 2016

DOI: 10.1021/acs.accounts.6b00329

changes,[23] ligand−receptor binding,[23] single virus particles,[20] antibody−antigen interactions,[31] and even neuronal activity.[32] Carbon nanotubes, graphene, and other silicon based biological sensors too have also shown similar detection capabilities for biologically relevant species like proteins,[33,34] DNAs,[35] glucose,[36] and living cells.[37]

All of the above-mentioned chemical and biological sensors have one thing in common−they rely on charge transfer between the adsorbed molecules and the nanomaterial which changes the surface charge density, thus altering the conductance of the sensors (Figure 1a). Although such charge-detection based sensing mechanisms provide label-free detection, high sensitivity, and electronic read-out, they have limited operational capability in practical vapor and solution based sensing environments. First, for gas sensing, DC sensors face the intrinsic speed-sensitivity trade-off due to the fact that vapor molecules are charge neutral and have poor interaction with a pristine nanosurface.[38] Charge transfer is possible only with selected molecules with large binding energy or at defect sites.[28] Unfortunately, the high binding energy leads to extremely slow sensing response and recovery, typically on the order of tens to thousands of seconds. Even low frequency capacitive and noise spectrum measurements suffer from poor sensitivity and slow response times (>100 s).[27] As a result, device regeneration requires prolonged heating,[26,39] degassing,[27] ultraviolet radiation,[40] current stimulation,[41] or chemo-selective coating;[24] all of which are impractical for robust on-site vapor monitoring systems. On the other hand, charge-detection based biological sensors fail in high background salt concentrations where device sensitivity suffers from Debye screening effect due to mobile ions present in the solution.[42,43] DC or low-frequency excitation signals cannot probe beyond the electrical double layer (EDL) formed by counterions, which is ∼1 nm for physiologically relevant conditions (∼100 mM). Consequently, most conventional nanoelectronic biosensors either operate in dry to low ionic buffer (<10 mM) conditions, or require complex preprocessing steps of desalting,[19] chemical modification of receptors,[44] or polymer coating of sensors,[45] all of which impede real-time point-of-care (POC) applications.

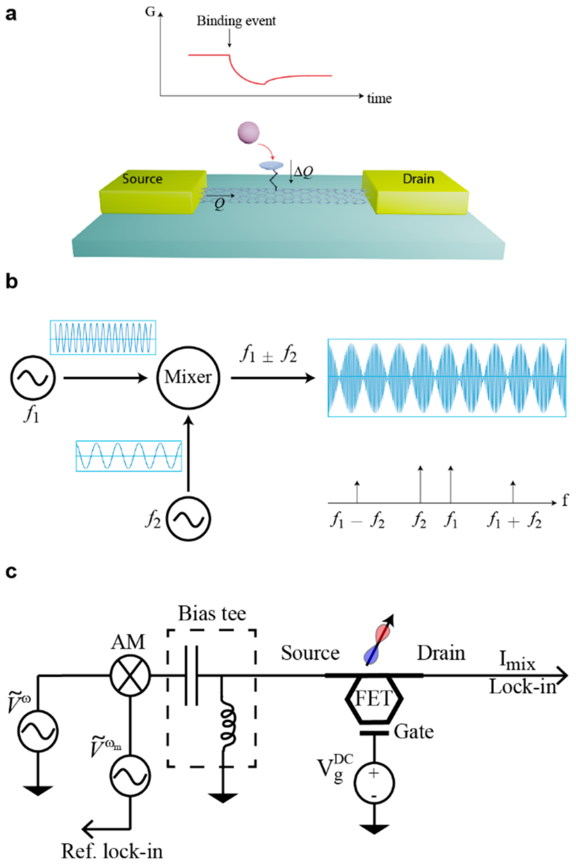

Figure 1. (a) Illustration of conventional charge-detection based measurement technique. (b) Concept of heterodyne mixing of two different frequency signals. (c) "One-source" heterodyne mixing measurement setup with AM modulated source excitation. A molecular dipole is shown on top of transistor. Reproduced with permission from ref 50. Copyright 2015 University of Michigan.

The above drawbacks are inherent to the DC measurement technique. Hence, the development of electronic sensor calls for a new sensing platform to counter the above-mentioned fundamental challenges. In our lab, we have developed a new sensing technology based on heterodyne mixing to investigate the interaction between charge density fluctuations in a nanoelectronic sensor caused by the oscillating dipole moment of molecule and an alternating current drive voltage which excites it.[46−50] By detecting the molecular dipole instead of charge, we address the fundamental speed-sensitivity trade-off issue and the ionic screening effect associated with conventional charge-detection based biosensors. Further, we have demonstrated that heterodyne sensing is platform independent and provides a versatile technology for detection in both liquid and gas phases.

THE PRINCIPLE OF NANOELECTRONIC HETERODYNE SENSOR

Heterodyne detection is based on the principle of mixing two different frequency signals to yield new signals at the sum and difference of the input frequencies (Figure 1b). It is commonly used in radio communications[51] and optical detection[52,53] where transmission/probing happens at high frequency, while detection is carried out at the down-converted difference frequency below the detection bandwidth of the detector. In addition, the mixing current measurement has also been explored in characterization of nanoelectronic and electromechanical devices.[54,55]

To understand heterodyne mixing in nanoelectronic sensors, we first consider the general expression of current signal for any nanoelectronic device given by

$$I = (G + \tilde{G}^{\omega})(V + \tilde{V}^{\omega}) = GV + G\tilde{V}^{\omega} + \tilde{G}^{\omega}V + \tilde{G}^{\omega}\tilde{V}^{\omega} \tag{1}$$

Here, G is the conductance, determined by charge density of the device, Q; $\tilde{G}^{\omega}$ is the conductance fluctuation related to charge density modulation, $\tilde{G}^{\omega}$; V is the direct current (DC) voltage, and $\tilde{V}^{\omega}$ is the alternating current (AC) excitation at frequency, $\omega/2\pi$. The change of I as the result of molecular binding gives the electronic sensor response. The first three terms of eq 1 give an insight into the various sensing methodologies that have been applied for nanoelectronic chemical and biological detection until date. The most common DC detection techniques monitor the first term GV;[17−23,26,28,30,32−36,38−40,43,44] the AC capacitive or impedance sensing techniques measures the second term, $G\tilde{V}^{\omega}$;[24,25,29,37,45] and the third term, $\tilde{G}^{\omega}V$ can be utilized for the low frequency noise sensing technique.[27,31] In contrast, it is the fourth term, $\tilde{G}^{\omega}\tilde{V}^{\omega}$ which explores the heterodyne mixing

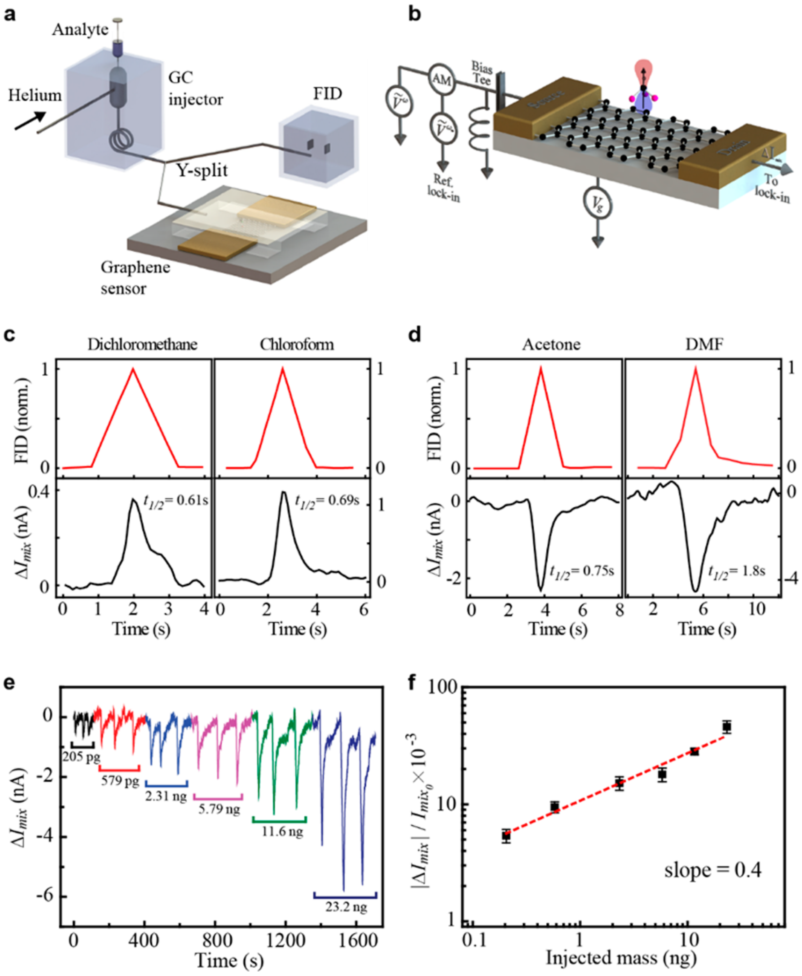

Figure 2. (a) Experimental setup showing a GC injector connected to the graphene sensor and a FID through a GC separation column and a Y-split. (b) Schematic showing a Gr-FET configured as a high-frequency mixer for heterodyne vapor sensing with a chloroform molecule on top. (c, d) Comparison of the temporal response of the FID (red) and a graphene sensor (black) to the same injected mass of four analytes (dichloromethane, 66.5 ng; chloroform, 296 ng; acetone, 15 ng; and DMF, 4.72 ng). (e) Chromatographic response of the sensor to repeated pulses of DMMP at varying mass injections. (f) Relative mixing current change of graphene sensor to DMMP mass injections obtained from (e). Linear fit (red line) to the log–log plot gives a slope of 0.4. Reproduced with permission from ref 48. Copyright 2014 Nature Publishing Group.

signal, I_{mix}, between conductance modulation and AC excitation and is the focus of this article. The heterodyne signal is dependent on the molecule's dipole moment and hence not affected by the fundamental challenges associated with charge-detection based DC sensors. Unfortunately, heterodyne sensing has been ignored until date in electronic sensing mainly due to the lack of gain in conventional two-terminal devices.

To implement heterodyne sensing technique, as one example, we use a three-terminal FET device structure in the "one-source" measurement scheme[56] (Figure 1c). The high-frequency signal applied to the source terminal of the FET provides both the frequency excitations for heterodyne mixing: one through the perturbation of molecular dipoles and second, through the excitation of nanomaterial channel. The conductance modulation, $\tilde{G}^{\omega}$ arises due to charge modulation in the nanomaterial and can be represented as, $\tilde{G} = \frac{dG}{dQ}\tilde{Q}$. The charge can be modulated through an external perturbation (i.e., absorbed molecule effect), $\tilde{Q}_{ext}$ or applied gate voltage, $\tilde{V}_g^{\omega}$. Therefore, the heterodyne mixing term from eq 1 can be written as

$$I_{mix} = \frac{dG}{dQ}(\tilde{Q}_{ext} + C_g\tilde{V}_g^{\omega})\tilde{V}^{\omega} \tag{2}$$

The term $\frac{dG}{dQ}$ is directly tied to the transconductance ($g_m = \frac{dG}{dV_g^{DC}}$) of the FET, which is defined as the ratio of change in output current ($I_{dc} = GV$) to the change in the input voltage ($V_g = \frac{Q}{C_g}$) of the FET. More importantly, this term represents the in situ gain/amplification for an FET, and in our case the mixing signal. The first term in the parentheses of eq 2 is of interest to us and represents the heterodyne response of a sensor due to the presence of molecules in the immediate environment of the sensor surface. The second term just represents the baseline mixing current signal. When a high frequency AC drive voltage is applied to the source terminal, it causes a perturbation of adsorbed molecules' dipole which in turn induces a charge-density modulation in the nanomaterial. This conductance modulation frequency-mixes with the AC excitation, thus generating the heterodyne mixing current. In our measurements, we use an amplitude modulated (AM) excitation voltage (typical carrier frequency parameters: $|\tilde{V}^{\omega}|$ =

Table 1. Summary of 13 Vapor Analytes Tested Using Graphene Heterodyne Sensors

analyte	dipole moment (D)	Smallest injected mass (ng)	fwhm (s) (averaged over triplicates)	concn at minimum injected mass (ppm)
pentane	0			
hexane	0			
benzene	0			
toluene	0.37	172	1.61	210
1,4-dioxane	0.45	52	2.1	50
chloroform	1.04	74	0.68	164
chlorobenzene	1.54	5.5	0.75	12
dichloromethane	1.6	66	1	139
2-propanol	1.66	39	1.12	105
ethanol	1.69	15	0.9	65
acetone	2.88	15	0.8	58
DMMP	3.62	0.205	6.83	0.043
DMF	3.82	0.944	2.54	0.92

10−20 mV, f_c = 100 kHz, and typical modulation signal parameters: $|\tilde{V}^{\omega_m}|$ = 1 V, f_m = 1.4342 kHz) to provide better noise rejection and detect the sensor response at the modulation reference frequency using a lock-in amplifier. In the following sections, we will demonstrate how heterodyne sensing not only provides rapid and sensitive chemical[48] and biological[46,47] detection, but also a sensitive probe to investigate, quantify, and even control fundamental molecule-nanomaterial interaction dynamics.[49]

NANOELECTRONIC HETERODYNE SENSORS FOR VAPOR SENSING

To demonstrate rapid and sensitive heterodyne vapor detection,[48] we fabricated graphene FETs (Gr-FETs) on silicon oxide/silicon wafer. The active graphene channel varied from 1 to 9 μm in length and 1−5 μm in width. The sensors were capped with a microfabricated silicon flow channel and connected to a standard gas chromatography (GC) system[57] using a simple GC guard column to deliver various analytes. Further, we use industry standard flame ionization detection (FID) for benchmarking sensor's speed and sensitivity. The entire measurement setup is shown in Figure 2a, and the frequency-mixing measurement schematic is illustrated in Figure 2b.

When vapor molecules adsorb on graphene surface, the source AC drive excites the molecular dipoles in the adsorbed layer. These oscillating dipoles act as a modulating gate potential at the same frequency as drive voltage, leading to a mixing current term, which is monitored. Significantly, the graphene heterodyne sensor shows simultaneously excellent sensitivity and speed. Figure 2c, d shows graphene heterodyne sensor's temporal response (in black) to four representative analytes. Subsecond full-width-half-maximum ($t_{1/2}$) response times were observed for dichloromethane ($t_{1/2}$ = 0.61 s), chloroform ($t_{1/2}$ = 0.69 s), and acetone ($t_{1/2}$ = 0.75 s) which were similar to or faster than FID response times (Figure 2c, d in red). Even relatively high boiling point vapors e.g. Dimethylformamide (DMF) showed response times ($t_{1/2}$ = 1.8 s) comparable to the FID.

Along with fast response, graphene heterodyne sensor exhibits high sensitivity, too. Figure 2e shows the sensor response to repeated doses of dimethyl methylphosphonate (DMMP) varying from 205 pg to 23.2 ng. The responses are instantaneous and completely reversible, with the lowest injected mass detected of 205 pg (limited by the instrument) corresponding to a concentration of approximately 43 ppb. Further, the log−log plot of sensor dosage in Figure 2f reveals a minimum detection limit of approximately 3 pg or 0.64 ppb in concentration, which to our knowledge is the lowest for any uncoated, pristine nanoelectronic vapor sensor. Our order of magnitude calculation suggests that the noise floor corresponds to ~10^4 molecules on the graphene surface (~10 μm^2) which can be further pushed down to <100 molecules by FET-sensor optimization. In Table 1 we list 13 analytes which were systematically investigated for response times and limits of detection (LOD). The high-frequency heterodyne detection provides superior performance compared to DC conductance measurement on the same Gr-FET sensor under similar excitation voltages,[48] as it (i) is more than an order-of-magnitude sensitive than DC response, (ii) is completely reversible, (iii) has much faster response and recovery times than DC response, and (iv) has lower noise levels.

For any practical real-time on-site vapor monitoring system, rapid separation and detection of analytes is critical. To demonstrate this, we investigate the heterodyne sensor response to a mixture of eight analytes which are separated using a combination of columns and delivered simultaneously to graphene sensor and FID using a Y-split (Figure 3). Graphene heterodyne sensor not only responds instantaneously to all polar molecules in the same temporal window as the FID, but also switches sign rapidly for molecules with different dipole orientation (electronegative and electropositive) relative to graphene, delivered one after the other.

PROBING THE MOLECULAR PHYSISORPTION DYNAMICS

Nanoelectronic systems are perfect platforms[13−16] to study and mimic the physicochemical nature of noncovalent interactions which, though weak in nature (~100s of meV;[58] Figure 4a), form the bedrock of most biological and cellular processes.[59] Unfortunately, the response of existing nanoelectronic systems is dominated by charge-transfer (covalent interactions) which does not represent the true interaction between charge neutral molecules and a pristine nanosurface. Here, nanoelectronic heterodyne sensors with their fast, sensitive and reversible responses allow us to monitor vapor kinetics near a nanomaterial surface in real-time and reveal the dynamics of their interaction. The noncovalent physisorption binding energy of a molecule to nanosurface is determined by the minima of potential energy formed by the competing electronic repulsive forces and attractive van der Waals forces.[58] Temperature control can impart enough thermal energy to

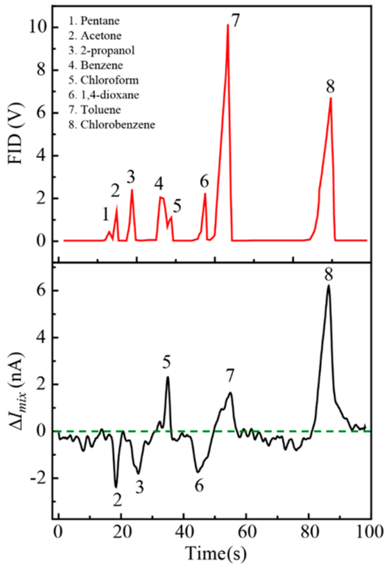

Figure 3. GC chromatograms obtained simultaneously from the FID (red) and the graphene sensor (black; L = 2 μm, W = 2 μm) for a mixture of 8 analytes delivered through a combination of columns and a Y-split. Reproduced with permission from ref 48. Copyright 2014 Nature Publishing Group.

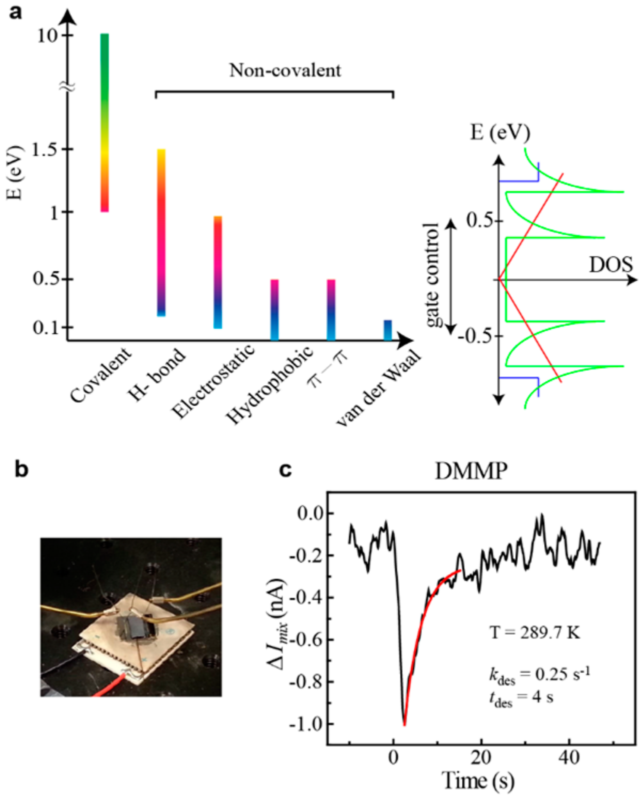

Figure 4. (a) Energy scales for covalent and noncovalent molecular interactions. Plotted on right is density of states for carbon nanotube (green), graphene (red), and MoS_2 (blue) versus energy. (b) Temperature-dependent measurement setup with device secured on top of a solid state cooler (white base). (c) Gr-FET temporal response to DMMP at 289.7 K. Exponential fit (in red) to desorption curve yields desorption rate k_{des} = 0.25 s^{-1} (τ_{des} = 4 s). Reproduced with permission from ref 49. Copyright 2016 American Chemical Society.

overcome this energy barrier providing a tool to quantify the binding energy. Further, the ability to electrically tune the charge density (hence the chemical potential) in nanomaterials via an electrostatic gate provides another parameter to enhance or weaken the electronic repulsion and control such fundamental interactions (Figure 4a, right).

We probe vapor molecule-nanomaterial interaction kinetics in real-time and quantify the thermodynamic binding affinities on a graphene nanoelectronic heterodyne platform using temperature-dependent desorption spectroscopy. For temperature-dependent desorption measurement, the heterodyne sensors were mounted on top of a solid state cooler, the temperature of which was controlled using a DC power supply (Figure 4b). The typical heterodyne response of DMMP molecules is illustrated in Figure 4c where the fast desorption curve can be fit with an exponential to obtain the desorption rate, k_{des} or desorption time, τ_{des} ($k_{des} = 1/\tau_{des}$) following first order rate kinetics, $r_{des} = A\,e^{-k_{des}t}$. From the transition state theory,[60] the molecular desorption process is governed by

$$k_{des} = \nu_f\, e^{-(E_a/k_BT)} \qquad (3)$$

where ν_f is the attempt frequency, E_a is the adsorbate binding energy, k_B is the Boltzmann constant, and T is the temperature. Hence, obtaining temperature-dependent molecular desorption rates can help quantify the thermodynamic binding energy. For example, Figure 5a represents the normalized heterodyne response of Gr-FET to DMMP at different temperatures where we observe faster molecular desorption at higher temperatures.

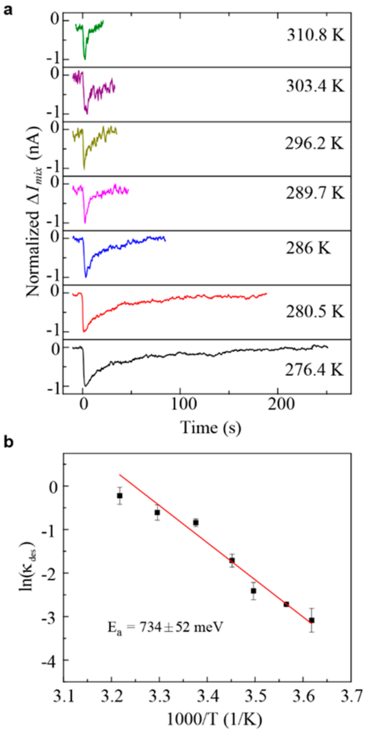

Figure 5. (a) Normalized temporal response of graphene mixer to 1.145 ng of DMMP at different temperatures. (b) Desorption rates, k_{des} obtained by exponential fit to graphene mixer's response to repeated doses of 1.145 ng DMMP plotted with temperature on Arrhenius scale. Slope (red) gives a noncovalent binding energy of 734 ± 52 meV. Error bars in b show the standard deviation over 3 runs. Reproduced with permission from ref 49. Copyright 2016 American Chemical Society.

DOI: 10.1021/acs.accounts.6b00329
Acc. Chem. Res. XXXX, XXX, XXX−XXX

To obtain the thermodynamic binding energies, Gr-FET response to repeated doses of DMMP were analyzed at different temperatures and the corresponding rate constants obtained through exponential fits were plotted with temperature on the Arrhenius scale as shown in Figure 5b. The slope of the Arrhenius plot yields a binding energy of 734 ± 52 meV for DMMP on graphene (Figure 5b).

Table 2 summarizes the experimentally obtained binding energies of six different molecules on graphene, including polar aromatic molecules which *π-stack* onto graphene, along with their dipole moments and polarizability values. Though the mixing current response relates to the molecular adsorbates' dipole moment, the binding energy is affected by both, dipole moment and polarizability of the molecules, since van der Waals forces include contributions from both.[58] In all temperature-dependent measurements, we observe a fall in Gr-FET peak response values at higher temperatures which agrees with the thermodynamic picture; i.e., the process becomes less spontaneous at higher temperature as both enthalpy and entropy also fall when molecules adsorb onto a surface (Gibbs free energy, $\Delta G = -|\Delta H| + T|\Delta S| > 0$).

Table 2. Experimental Binding Energy ($E_{\text{bind}}^{\text{exp}}$, meV), Dipole Moment ($D$, Debye), Polarizability (α, 10^{-24} cm^3) and Graphene's Fermi Level Offset from the Dirac Point (ΔE_{F}^{0}, meV) for Six Different Molecules Studied

analyte	D	α	$E_{\text{bind}}^{\text{exp}}$	ΔE_{F}^{0}
chloroform	1.04	8.23	223 ± 13	−160
dichloromethane	1.6	6.48	195 ± 10	−250
chlorobenzene	1.54	12.3	367 ± 30	−240
1,2 dichlorobenzene	2.5	14.17	447 ± 24	−250
DMMP	3.62	10	734 ± 52	−220
DMF	3.82	7.8	657 ± 23	−150

Further, graphene also provides a continuous range of gate tunable Fermi energies[61] making it an ideal platform to demonstrate electrical tuning of noncovalent interactions. In Figure 6a and b, we show that, by changing the gate voltage, the molecular desorption of chloroform and DMF can be altered. We observe that more positive gate voltages and higher Fermi levels weaken chloroform physisorption on graphene, leading to a higher desorption rate and lower mixing current peaks. On the other hand, the gate control on DMF physisorption is opposite where positive gate voltages enhance the interaction between DMF and graphene molecules. The opposite trend for the gate tuning of chloroform and DMF desorption is due to their opposite dipole orientations on top of graphene.[48] Significantly, this is the first time that electrical tuning of molecular physisorption has been demonstrated dynamics where molecular desorption on graphene can be slowed down nearly 3 times within a gate voltage range of 15 V (Figure 6c, d).

NANOELECTRONIC HETERODYNE BIOSENSORS

At DC or low frequency, ions in solution migrate toward the charged surface forming an EDL and screening off the target molecules, which can be several nanometers from the nanosurface.[18] In this section, we demonstrate how heterodyne sensing can be employed to mitigate ionic screening effect at high frequencies when ions in solution cannot follow the AC driving field and do not have sufficient time to form the EDL.

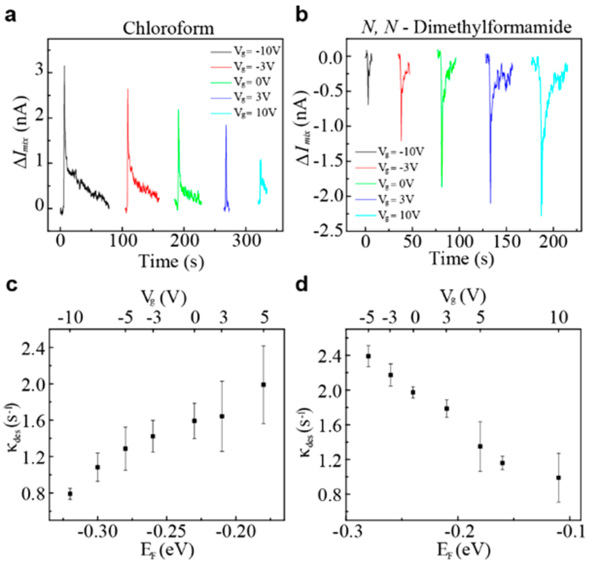

Figure 6. Mixing current response at room temperature for (a) chloroform (285 ng) and (b) DMF (18.88 ng) at different back-gate voltages. Desorption rates, k_{des}, obtained from exponential fits to the mixing current responses to repeated doses of (c) chloroform and (d) DMF, respectively, plotted against graphene Fermi level shift and applied gate voltage. Error bars in (c) and (d) show the standard deviation over three runs. Reproduced with permission from ref 49. Copyright 2016 American Chemical Society.

Figure 7a shows the heterodyne biosensor setup which is implemented on a single-walled carbon nanotube (SWNT) field-effect-transistor platform. We use a suspended top-gate architecture as shown in Figure 7a where the nanotube is exposed to the solution for sidewall modification and biodetection, and also allows for a compact microfluidic seal. We chose the biotin–streptavidin ligand–receptor system to evaluate the sensing capability of our biosensor in different background ionic strengths.

The low frequency range, f (200 kHz–1 MHz) dependence of the peak mixing currents for DI water, 1 mM, 10 mM and 100 mM solution backgrounds are presented in Figure 7b–e. The peaks are the point of maximum nonlinearity (hence, maximum transconductance) in the electrical characteristics. As the background ionic strength increases from DI water (screening length ∼ 1 μm) to 100 mM NaCl (screening length ∼ 1 nm), we observed that differences in I_{mix} before and after streptavidin binding became smaller and smaller, and finally vanished in 100 mM NaCl, confirming the Debye screening of streptavidin–biotin complex. To mitigate this, we operate our carbon nanotube FET sensors at higher frequencies.[62] Figure 8a shows the $I_{\text{mix}} - V_g$ characteristics of the same SWNT-FET in 100 mM NaCl at f = 10 MHz before and after streptavidin binding. We observe that the FET-sensor recovered its sensitivity beyond f > 1 MHz as can be seen in both the amplitude and phase of peak sensor response (Figure 8b), and a maximum relative sensitivity ($\Delta I_{\text{mix}}/I_{\text{mix}}$) of 25% was observed at f = 10 MHz (Figure 8c). The recovery of sensitivity is caused by the breakdown of the EDL[62] when at high frequency, the ions in solution experience a lag due to their finite diffusivity and are unable to follow the excitation field. As the EDL is weakened, the AC electric field penetrates deeper into the solution, and can drive the dipoles of streptavidin–biotin complex. The MHz sensitivity-recovery frequency agrees

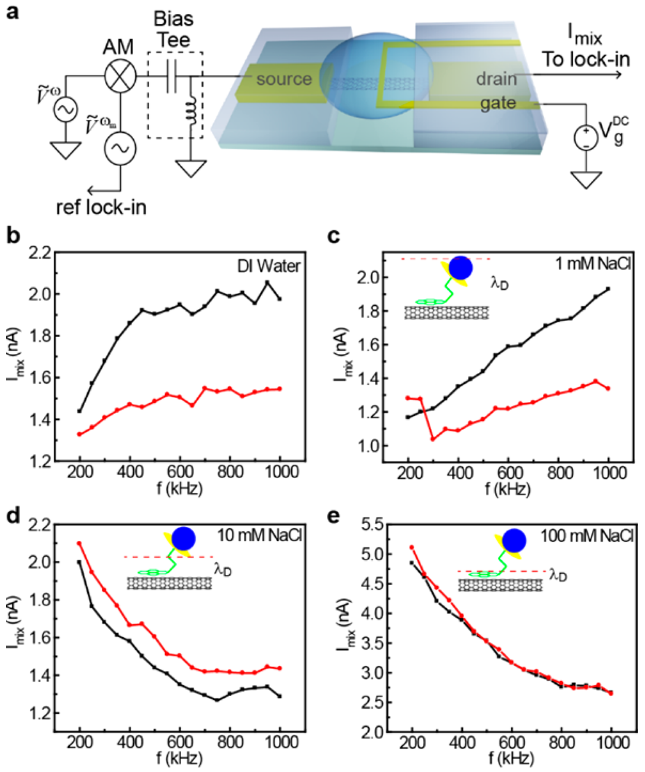

Figure 7. (a) Carbon nanotube heterodyne biosensor measurement setup. (b−e) Peak I_{mix} values are plotted over 200 kHz−1 MHz for before (black) and after (red) streptavidin−biotin binding in (a) DI water, (b) 1 mM NaCl, (c) 10 mM NaCl, and (d) 100 mM NaCl background solutions. Insets in (b)−(d) illustrate Debye lengths compared to biomolecule separation from sensor surface. Reproduced with permission from ref 46. Copyright 2012 American Chemical Society.

with the estimated relaxation time ($10^{-7} \leq \tau_0 \leq 10^{-5}$) for EDL.[62]

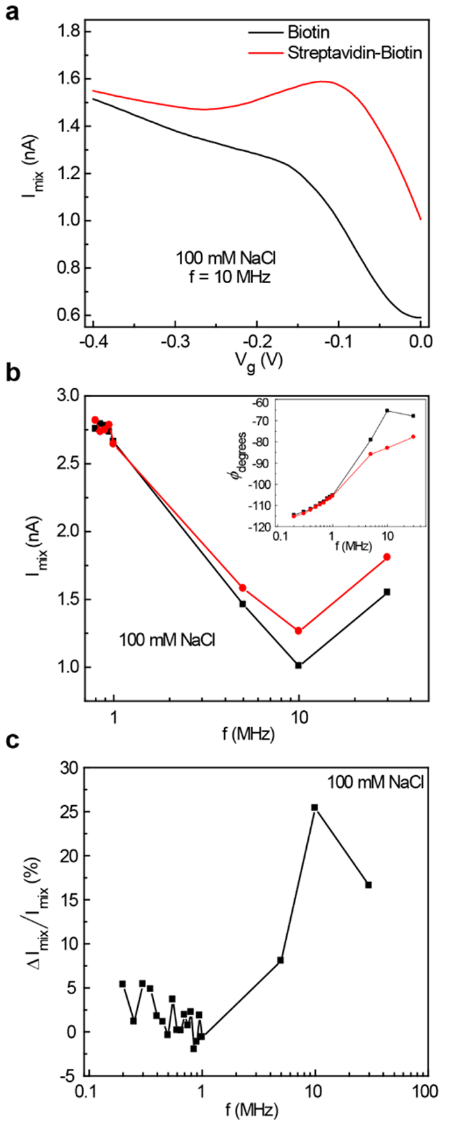

Figure 8. (a) I_{mix} − V_g curves before (black) and after (red) streptavidin−biotin binding in 100 mM NaCl at f = 10 MHz. (b) Peak I_{mix} values plotted from 800 kHz−30 MHz for both before (black) and after streptavidin binding (red) in 100 mM NaCl. Inset: Phase information on I_{mix}. (c) Relative sensitivity, $\Delta I_{mix}/I_{mix}$ of high frequency SWNT sensor versus f. Reproduced with permission from ref 46. Copyright 2012 American Chemical Society.

■ CONCLUSIONS AND FUTURE DIRECTIONS

Although electronic sensors promise high sensitivity, are convenient to use, and provide compatibility with modern semiconductor technology, the current dominant technologies for chemical and biological sensors are still optics based. Addressing the fundamental challenges facing current electronic sensing technologies calls for new sensing paradigms. For the past several years, we are tiptoeing in the new direction of nanoelectronic heterodyne sensing using carbon nanotube and graphene FETs. By exploring the heterodyne mixing current between AC excitation and molecular dipole induced conductance oscillation, our heterodyne sensors overcome some of the fundamental challenges facing conventional DC chemical and biological sensors. We demonstrate that nanoelectronic heterodyne sensors fulfill the critical criteria for practical vapor monitoring setups, namely, speed, sensitivity, size, stability, and broad spectrum detection, and promise the development of highly integrated, rapid, and sensitive chemical sensors. Furthermore, heterodyne sensing technique can also be used for the experimental study of noncovalent molecule-nanomaterial interactions. In particular, the electrical tuning of interaction dynamics between small molecules and graphene adds another dimension to engineer chemical control-on-chip which has potential applications in diverse fields ranging from biochemical recognition to catalysis. The heterodyne sensing technique can also be an important technique for biosensing in solution. Ionic screening is one of the fundamental reasons why nanoelectronic biosensors, even after a decade of research and investigation, have not found wide applicability. Our work is the first such report to demonstrate biological detection directly in high ionic backgrounds.

We firmly believe nanoelectronic heterodyne sensing can revolutionize point-of-need chemical and biomolecular analyses. Our work has mainly concentrated on carbon nanomaterial platforms which have the advantages of chemically inert surface, true nanometer dimension, and exceptional electronic properties. However, there is no reason why this technique cannot be readily adopted onto other material platforms, including various low dimensional materials and more conventional bulk semiconductors such as silicon. Though heterodyne detection is a new paradigm for electronic sensing, we want to point out certain challenges and future research avenues that need to be investigated for wider applicability of this technique and ultimately, electronic sensors. First, the detection of nonpolar molecules can be challenging for both heterodyne sensors and conventional DC sensors. It is possible to address this issue by exploring the molecular polarizability and the imperfect screening of the semimetallic graphene sheet. Second, sensing specificity is another challenge for electronic sensors in general. Selectivity can be introduced through analyte-specific chemical functionalization on graphene or other nanosensor surface. It may also be possible to explore the intrinsic dipole resonance of target molecules for a true label-free detection by pushing the excitation frequency into GHz regime. Finally, water molecule has large dipole moment and the resulting dielectric screening effect could limit the sensitivity of a heterodyne biosensor. It is possible overcome the dielectric screening from water by going beyond water molecule's dipole resonance frequency.

AUTHOR INFORMATION

Corresponding Author

*E-mail: zzhong@umich.edu.

Notes

The authors declare no competing financial interest.

Biographies

Girish Kulkarni received his Ph.D. in Electrical Engineering from University of Michigan Ann Arbor working on carbon nanomaterial based chemical and biological sensors. Currently, he is a Research Fellow at University of Michigan and the President of Arborsense Inc., a startup company funded by National Science Foundation and developing nanoelectronic sensors for healthcare applications.

Wenzhe Zang obtained her B.S. in Chemistry from Nanjing University, China (2013). During her undergraduate, she investigated nanostructure synthesis and 2D material functionalization. She is now pursuing her Ph.D. degree in Electrical Engineering at University of Michigan under the guidance of Prof. Zhaohui Zhong. Her current research interests focus on development of novel nanoelectronic sensor for chemical and biological detection.

Zhaohui Zhong is currently an Associate Professor of Electrical Engineering and Computer Science at the University of Michigan. He received his B.S. and M.S. in Chemistry from Nanjing University in 1998 and 2000, and his Ph.D. in Chemistry from Harvard University in 2005. From 2005 to 2008, he was a postdoctoral associate at Cornell University Center for Nanoscale Systems. He joined the faculty of EECS at the University of Michigan in 2008. He is a recipient of NSF CAREER award. His research lies at the frontiers of nanoelectronics and nanophotonics.

ACKNOWLEDGMENTS

The authors acknowledge the support from National Science Foundation under ECCS-1405870 and DMR-1120187 grants.

REFERENCES

(1) Lim, D. V.; Simpson, J. M.; Kearns, E. A.; Kramer, M. F. Current and developing technologies for monitoring agents of bioterrorism and biowarfare. *Clin. Microbiol. Rev.* **2005**, *18*, 583−607.

(2) Ho, C. K.; Robinson, A.; Miller, D. R.; Davis, M. J. Sensors for Environmental Monitoring and Long-Term Environmental Stewardship. *Sandia Report*; Sandia National Laboratories: Albuquerque, NM, 2004.

(3) Dawson, E.; Moore, C.; Dankbar, D.; Mehlmann, M.; Townsend, M.; Smagala, J.; Smith, C.; Cox, N.; Kuchta, R.; Rowlen, K. Identification of A/H5N1 influenza viruses using a single gene diagnostic microarray. *Anal. Chem.* **2007**, *79*, 378−384.

(4) Ligler, F.; Erickson, J. Bioengineering - Diagnosis on disc. *Nature* **2006**, *440*, 159−160.

(5) Ketteler, R.; Sun, Z.; Kovacs, K. F.; He, W.; Seed, B. A pathway sensor for genome-wide screens of intracellular proteolytic cleavage. *Genome Biol.* **2008**, *9*, R64.

(6) Deo, S.; Moschou, E.; Peteu, S.; Eisenhardt, P.; Bachas, L.; Madou, M.; Daunert, S. Responsive drug delivery systems. *Anal. Chem.* **2003**, *75*, 206A−213A.

(7) Madou, M. J.; Cubicciotti, R. Scaling issues in chemical and biological sensors. *Proc. IEEE* **2003**, *91*, 830−838.

(8) Bergstrom, P. L. A microfabricated work-function gas sensor for semiconductor process gas detection. Ph.D. Thesis, University of Michigan, Ann Arbor, MI, 1996.

(9) Bănică, F.-G. *Chemical sensors and biosensors: fundamentals and applications*; John Wiley and Sons: Chichester, UK, 2012.

(10) Zhang, A.; Lieber, C. M. Nano-Bioelectronics. *Chem. Rev.* **2016**, *116*, 215−257.

(11) Kauffman, D. R.; Star, A. Carbon nanotube gas and vapor sensors. *Angew. Chem., Int. Ed.* **2008**, *47*, 6550−6570.

(12) Arjmandi-Tash, H.; Belyaeva, L. A.; Schneider, G. F. Single molecule detection with graphene and other two-dimensional materials: nanopores and beyond. *Chem. Soc. Rev.* **2016**, *45*, 476−493.

(13) Lu, W.; Lieber, C. M. Nanoelectronics from the bottom up. *Nat. Mater.* **2007**, *6*, 841−850.

(14) Geim, A. K.; Novoselov, K. S. The rise of graphene. *Nat. Mater.* **2007**, *6*, 183−191.

(15) McEuen, P. L.; Fuhrer, M. S.; Park, H. K. Single-walled carbon nanotube electronics. *IEEE Trans. Nanotechnol.* **2002**, *1*, 78−85.

(16) Wang, Q.; Kalantar-Zadeh, K.; Kis, A.; Coleman, J.; Strano, M. S. Electronics and optoelectronics of two-dimensional transition metal dichalcogenides. *Nat. Nanotechnol.* **2012**, *7*, 699−712.

(17) Zhang, D.; Liu, Z.; Li, C.; Tang, T.; Liu, X.; Han, S.; Lei, B.; Zhou, C. Detection of NO2 down to ppb levels using individual and multiple In2O3 nanowire devices. *Nano Lett.* **2004**, *4*, 1919−1924.

(18) Stern, E.; Klemic, J. F.; Routenberg, D. A.; Wyrembak, P.; Turner-Evans, D. B.; Hamilton, A. D.; LaVan, D.; Fahmy, T. M.; Reed, M. A. Label-free immunodetection with CMOS-compatible semiconducting nanowires. *Nature* **2007**, *445*, 519−522.

(19) Zheng, G.; Patolsky, F.; Cui, Y.; Wang, W.; Lieber, C. M. Multiplexed electrical detection of cancer markers with nanowire sensor arrays. *Nat. Biotechnol.* **2005**, *23*, 1294−1301.

(20) Patolsky, F.; Zheng, G.; Hayden, O.; Lakadamyali, M.; Zhuang, X.; Lieber, C. M. Electrical detection of single viruses. *Proc. Natl. Acad. Sci. U. S. A.* **2004**, *101*, 14017−14022.

(21) Kong, J.; Dai, H. Full and modulated chemical gating of individual carbon nanotubes by organic amine compounds. *J. Phys. Chem. B* **2001**, *105*, 2890−2893.

(22) Star, A.; Han, T. R.; Gabriel, J. C. P.; Bradley, K.; Gruner, G. Interaction of aromatic compounds with carbon nanotubes: Correlation to the Hammett parameter of the substituent and measured carbon nanotube FET response. *Nano Lett.* **2003**, *3*, 1421−1423.

(23) Cui, Y.; Wei, Q.; Park, H. K.; Lieber, C. M. Nanowire nanosensors for highly sensitive and selective detection of biological and chemical species. *Science* **2001**, *293*, 1289−1292.

(24) Snow, E.; Perkins, F.; Houser, E.; Badescu, S.; Reinecke, T. Chemical detection with a single-walled carbon nanotube capacitor. *Science* **2005**, *307*, 1942−1945.

(25) Alldredge, E.; Badescu, S.; Bajwa, N.; Perkins, F.; Snow, E.; Reinecke, T.; Passmore, J.; Chang, Y. Adsorption of linear chain molecules on carbon nanotubes. *Phys. Rev. B: Condens. Matter Mater. Phys.* **2008**, *78*, 161403.

(26) Schedin, F.; Geim, A. K.; Morozov, S. V.; Hill, E.; Blake, P.; Katsnelson, M. I.; Novoselov, K. S. Detection of individual gas molecules adsorbed on graphene. *Nat. Mater.* **2007**, *6*, 652−655.

(27) Rumyantsev, S.; Liu, G.; Shur, M. S.; Potyrailo, R. A.; Balandin, A. A. Selective Gas Sensing with a Single Pristine Graphene Transistor. *Nano Lett.* **2012**, *12*, 2294−2298.

(28) Kumar, B.; Min, K.; Bashirzadeh, M.; Farimani, A. B.; Bae, M.; Estrada, D.; Kim, Y. D.; Yasaei, P.; Park, Y. D.; Pop, E.; Aluru, N. R.; Salehi-Khojin, A. The Role of External Defects in Chemical Sensing of Graphene Field-Effect Transistors. *Nano Lett.* **2013**, *13*, 1962−1968.

(29) Perkins, F.; Friedman, A.; Cobas, E.; Campbell, P.; Jernigan, G.; Jonker, B. T. Chemical Vapor Sensing with Mono layer MoS2. *Nano Lett.* **2013**, *13*, 668−673.

(30) Kou, L.; Frauenheim, T.; Chen, C. Phosphorene as a Superior Gas Sensor: Selective Adsorption and Distinct I-V Response. *J. Phys. Chem. Lett.* **2014**, *5*, 2675−2681.

(31) Zheng, G.; Gao, X.; Lieber, C. M. Frequency Domain Detection of Biomolecules Using Silicon Nanowire Biosensors. *Nano Lett.* **2010**, *10*, 3179−3183.

(32) Patolsky, F.; Timko, B. P.; Yu, G.; Fang, Y.; Greytak, A. B.; Zheng, G.; Lieber, C. M. Detection, stimulation, and inhibition of neuronal signals with high-density nanowire transistor arrays. *Science* **2006**, *313*, 1100−1104.

(33) Bradley, K.; Briman, M.; Star, A.; Gruner, G. Charge transfer from adsorbed proteins. *Nano Lett.* **2004**, *4*, 253−256.

(34) Chen, R.; Zhang, Y.; Wang, D.; Dai, H. Noncovalent sidewall functionalization of single-walled carbon nanotubes for protein immobilization. *J. Am. Chem. Soc.* **2001**, *123*, 3838−3839.

(35) Star, A.; Tu, E.; Niemann, J.; Gabriel, J.; Joiner, C. S.; Valcke, C. Label-free detection of DNA hybridization using carbon nanotube network field-effect transistors. *Proc. Natl. Acad. Sci. U. S. A.* **2006**, *103*, 921−926.

(36) Huang, Y.; Dong, X.; Shi, Y.; Li, C.; Li, L.; Chen, P. Nanoelectronic biosensors based on CVD grown graphene. *Nanoscale* **2010**, *2*, 1485−1488.

(37) Laborde, C.; Pittino, F.; Verhoeven, H.; Lemay, S.; Selmi, L.; Jongsma, M.; Widdershoven, F. P. Real-time imaging of microparticles and living cells with CMOS nanocapacitor arrays. *Nat. Nanotechnol.* **2015**, *10*, 791−795.

(38) Dan, Y.; Lu, Y.; Kybert, N. J.; Luo, Z.; Johnson, A. T. C. Intrinsic Response of Graphene Vapor Sensors. *Nano Lett.* **2009**, *9*, 1472−1475.

(39) Li, J.; Lu, Y.; Ye, Q.; Cinke, M.; Han, J.; Meyyappan, M. Carbon nanotube sensors for gas and organic vapor detection. *Nano Lett.* **2003**, *3*, 929−933.

(40) Dua, V.; Surwade, S. P.; Ammu, S.; Agnihotra, S. R.; Jain, S.; Roberts, K. E.; Park, S.; Ruoff, R. S.; Manohar, S. K. All-Organic Vapor Sensor Using Inkjet-Printed Reduced Graphene Oxide. *Angew. Chem., Int. Ed.* **2010**, *49*, 2154−2157.

(41) Salehi-Khojin, A.; Lin, K.; Field, C. R.; Masel, R. I. Nonthermal Current-Stimulated Desorption of Gases from Carbon Nanotubes. *Science* **2010**, *329*, 1327−1330.

(42) Stern, E.; Wagner, R.; Sigworth, F.; Breaker, R.; Fahmy, T. M.; Reed, M. A. Importance of the debye screening length on nanowire field effect transistor sensors. *Nano Lett.* **2007**, *7*, 3405−3409.

(43) Nair, P. R.; Alam, M. A. Screening-limited response of nanobiosensors. *Nano Lett.* **2008**, *8*, 1281−1285.

(44) Elnathan, R.; Kwiat, M.; Pevzner, A.; Engel, Y.; Burstein, L.; Khatchtourints, A.; Lichtenstein, A.; Kantaev, R.; Patolsky, F. Biorecognition Layer Engineering: Overcoming Screening Limitations of Nanowire-Based FET Devices. *Nano Lett.* **2012**, *12*, 5245−5254.

(45) Gao, N.; Zhou, W.; Jiang, X.; Hong, G.; Fu, T.; Lieber, C. M. General Strategy for Biodetection in High Ionic Strength Solutions Using Transistor-Based Nanoelectronic Sensors. *Nano Lett.* **2015**, *15*, 2143−2148.

(46) Kulkarni, G. S.; Zhong, Z. Detection beyond the Debye Screening Length in a High-Frequency Nanoelectronic Biosensor. *Nano Lett.* **2012**, *12*, 719−723.

(47) Kulkarni, G. S.; Zhong, Z. Fabrication of Carbon Nanotube High-Frequency Nanoelectronic Biosensor for Sensing in High Ionic Strength Solutions. *J. Visualized Exp.* **2013**, No. 77, e50438.

(48) Kulkarni, G. S.; Reddy, K.; Zhong, Z.; Fan, X. Graphene nanoelectronic heterodyne sensor for rapid and sensitive vapour detection. *Nat. Commun.* **2014**, *5*, 4376.

(49) Kulkarni, G. S.; Reddy, K.; Zang, W.; Lee, K.; Fan, X.; Zhong, Z. Electrical Probing and Tuning of Molecular Physisorption on Graphene. *Nano Lett.* **2016**, *16*, 695−700.

(50) Kulkarni, G. S. Carbon nanoelectronic heterodyne sensors: A new paradigm for chemical and biological detection. Ph.D. Thesis, University of Michigan, Ann Arbor, MI, 2015.

(51) Hagen, J. B. *Radio-frequency electronics: circuits and applications*; Cambridge University Press: Cambridge, UK, 1996.

(52) Maznev, A. A.; Nelson, K. A.; Rogers, T. A. Optical heterodyne detection of laser-induced gratings. *Opt. Lett.* **1998**, *23*, 1319−1321.

(53) Strauss, C. E. M. Synthetic-Array Heterodyne-Detection - a Single-Element Detector Acts as an Array. *Opt. Lett.* **1994**, *19*, 1609−1611.

(54) Rosenblatt, S.; Lin, H.; Sazonova, V.; Tiwari, S.; McEuen, P. L. Mixing at 50 GHz using a single-walled carbon nanotube transistor. *Appl. Phys. Lett.* **2005**, *87*, 153111.

(55) Sazonova, V.; Yaish, Y.; Ustunel, H.; Roundy, D.; Arias, T. A.; McEuen, P. L. A tunable carbon nanotube electromechanical oscillator. *Nature* **2004**, *431*, 284−287.

(56) Sazonova, V. A. Tunable Carbon Nanotube Resonator. Ph.D. Thesis, Cornell University, Ithaca, NY, 2006.

(57) McNair, H. M.; Miller, J. M. *Basic Gas Chromatography*; John Wiley and Sons: Hoboken, NJ, 2009.

(58) Israelachvili, J. N. *Intermolecular and Surface Forces*, Third ed.; Academic Press: Waltham, MA, 2011.

(59) Frieden, E. Noncovalent Interactions - Key To Biological Flexibility And Specificity. *J. Chem. Educ.* **1975**, *52*, 754−761.

(60) Somorjai, G. A. *Introduction to surface chemistry and catalysis*; John Wiley and Sons: New York, 1994.

(61) Das Sarma, S.; Adam, S.; Hwang, E. H.; Rossi, E. Electronic transport in two-dimensional graphene. *Rev. Mod. Phys.* **2011**, *83*, 407−470.

(62) Bockris, J. O.; Gileadi, E.; Muller, K. Dielectric Relaxation in Electric Double Layer. *J. Chem. Phys.* **1966**, *44*, 1445−1456.

DOI: 10.1021/acs.accounts.6b00329
Acc. Chem. Res. XXXX, XXX, XXX−XXX